

Programmable manipulation of motile cells in optoelectronic tweezers using a grayscale image

Wonjae Choi,¹ Seong-Won Nam,² Hyundoo Hwang,¹ Sungsu Park,^{2,a)} and Je-Kyun Park^{1,b)}

¹Department of Bio and Brain Engineering, KAIST, 335 Gwahangno, Yuseong-gu, Daejeon 305-701, Republic of Korea

²Department of Chemistry and Nano Sciences (BK21), Ewha Womans University, Seodaemun-gu, Seoul 120-750, Republic of Korea

(Received 28 July 2008; accepted 17 September 2008; published online 6 October 2008)

This paper describes a grayscale optoelectronic tweezers (OET) which allows adjustment of the electric field strength at each position of OET. A grayscale light image was used to pattern vertical electric field strength on an OET. As an electric field depends on the brightness at each point, the brighter light patterns generate the stronger electric field in the OET. Its feasibility for application to cell manipulation was demonstrated by aligning highly motile protozoan cells in vertical direction. Depending on the brightness of each pixel, the behaviors of aligned cells varied due to the different electric field strength to each cell. © 2008 American Institute of Physics.

[DOI: 10.1063/1.2996277]

Optical manipulation techniques such as optical tweezers¹ have been used to study dynamic behaviors of motile cells.²⁻⁴ However, none of these technologies has been able to simultaneously apply different strength of force to individual cells. Recently, optoelectronic tweezers (OET) have emerged as a powerful tool for massively parallel manipulation of microparticles and living cells.⁵ This technology uses a photoconductive layer to allow an optical image to control the electric field and has been applied to the manipulation of living cells, microparticles, and nanoparticles.⁵⁻¹⁰ Until now, OET has been only operated by the binary optical image, which has two binary values (on/off transmission) for each pixel, and a control of the electric field strength at each pixel has not been exploited, while a change in the bias voltage causes a change in the scale of whole electric field.

Here we describe a grayscale OET, which allows adjustment of the electric field strength at each pixel using a grayscale image with a variable intensity value for each pixel. To demonstrate its functionality, we apply this technology to manipulate cells of the ciliated protozoan *Tetrahymena pyriformis* (*T. pyriformis*). The ciliates are known to swim by coordinating their ciliary beating.

The schematic configuration of the experimental setup of the grayscale OET is shown in Fig. 1. Overall setup consists of an OET device and a 0.5 in. liquid crystal display (LCD) module (L3P05S Series, Seiko Epson, Japan) installed in an upright microscope (Zeiss Axioskop 40, Carl Zeiss, Germany). In the OET part, a cell-containing solution was sandwiched between the photoconductive layer and the ground layer, and a double-sided adhesive tape was used as a spacer of 120 μm thick. Detailed procedures of the OET fabrication are elsewhere.^{7,11} Cell behaviors were observed and captured with a charge-coupled device camera (Pike F032C, Allied Vision Technologies, Germany). The brightness was measured using an illuminance meter (T-10M, Konica Minolta, Japan) and the bias voltage of 12 V_{pp} at 10 kHz was pro-

duced from a function generator (AGF3022, Tektronix, OR). A grayscale image was controlled by standard presentation software (Microsoft PowerPoint™) on a computer.

T. pyriformis were obtained from the American Type Culture Collection (ATCC, Manassas, VA) and were cultured in a medium containing 0.5% peptone and 0.5% tryptone and 0.02% K₂HPO₄ (w/v). Cells were centrifuged at 500 × *g* for 2 min to collect a high density of cells and suspended in the experimental buffer (phosphate buffered saline solution with a conductivity of 22 $\mu\text{S}/\text{cm}$).

In order to manipulate swimming cells by the OET, the cells were introduced to the liquid layer of the OET and a vertical electric field was applied between the photoconduc-

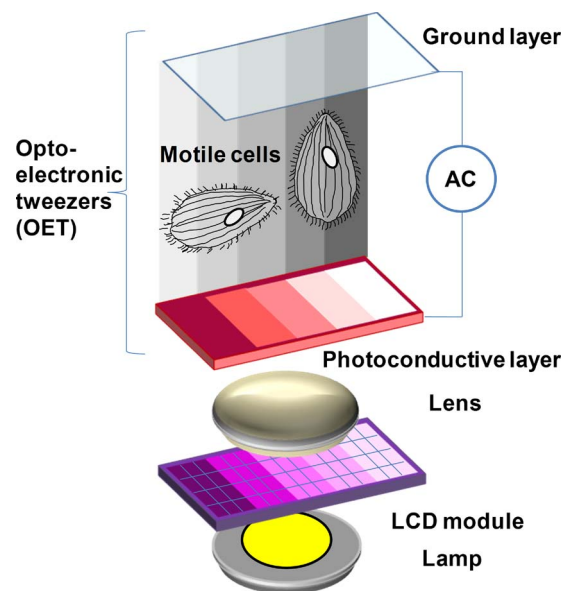


FIG. 1. (Color online) Experimental setup of grayscale OET for the alignment of swimming cells. *Tetrahymena* cells were introduced to the liquid layer of the OET device, which an electric field was applied. An LCD module made a grayscale image and transmit it to the photoconductive layer of the OET. At the region where the light intensity was high (the right side of the photoconductive layer), the electric field was strong and thus the cells were aligned.

^{a)}Electronic mail: nanopark@ewha.ac.kr.

^{b)}Electronic mail: jekyun@kaist.ac.kr.

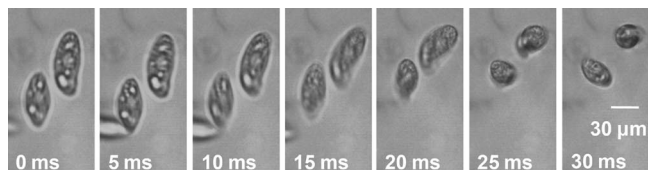


FIG. 2. Captured movie stills showing a typical alignment behavior of *T. pyriformis*. The vertical electric field across the liquid layer was $50 \text{ mV}_{\text{pp}}/\mu\text{m}$.

tive layer and the ground layer in the OET. In a control experiment with a grayscale image and without an electric field, the image pattern gave no apparent effect on the free swimming of the cells. This result implies that there is little effect by the light. In addition, we conducted another control experiment with a vertical electric field and without the image. A transparent electrode was used instead of the photoconductive layer in the OET device, and an electric bias of 6 V_{pp} at 10 kHz was applied to make proper vertical electric field strength of $50 \text{ mV}_{\text{pp}}/\mu\text{m}$. Figure 2 shows a sequence of still images showing a typical example of the cell alignment where cells were observed using a top view. It is inferred that the cells freely swim when there is no electric field. When an electric field was applied, however, the cells become oriented into a vertical direction and appeared to be trapped. However, their ciliary movements were still sustained (data not shown), thereby allowing the aligned cells to move in the vertical direction. Accordingly, the lateral movement of the vertically orientated cells was decreased.

Electro-orientation is the ability to align nonspherical particles immersed in a solution of different permittivity with an electric field. Compared to dielectrophoresis (DEP) or electrorotation, it is similar but different in many aspects.^{12,13} DEP occurs in a nonuniform field and electrorotation occurs in a rotating electric field, while electro-orientation occurs for nonspherical particle even in a uniform electric field. Electro-orientation was applied to the study of several types of cells such as red blood cells^{12,14} and bacteria.¹⁵ Recently, it was reported that electro-orientation occurred during the OET manipulations of nanowires⁹ and red blood cells.¹¹

Figures 3(a)–3(d) show a typical alignment behavior of swimming cells in the grayscale OET. The brightness of each pixel in the grayscale image was linearly increased from the left to the right (see Ref. 16). When there was a uniform dark image at 0 s, the cells at any position swam freely and looked as an elongated shape. However, as the image appeared gradually from 0 to 6 s, the cells at the bright region were aligned. These cells did not swim freely, vibrated at almost the same place and looked as a circular shape. According to the brightness of each pixel, cell alignment behaviors were different due to the different electric field. At the bright region, more cells were aligned than the cells at the dark region. When the image disappeared gradually from 8 to 14 s, the aligned cells got their original shape again and swam freely one after another. After the image disappeared all over, every cell swam freely and returned to its original elongated shape. In addition, there was no apparent damage of cells. The various strength of the electric field was also applied for each swimming cells at the same time and on the same stage. To measure the alignment ratios, the pattern of light image is designed to have five areas of different brightness (1677, 3140, 10 036, 24 722, and 43 872 lux)

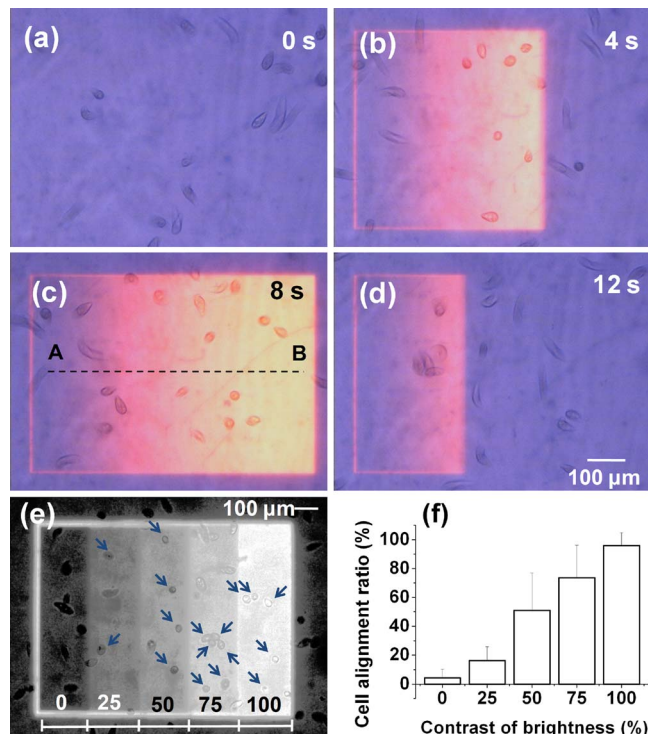


FIG. 3. (Color online) Cell alignment experiments of *T. pyriformis* using a grayscale OET. [(a)–(d)] Captured movie stills showing cell alignment in the grayscale OET. As an image with a gradient appeared from 0 to 6 s, the cells at the bright region were aligned. When the light image disappeared from 8 to 14 s, the cells swam freely again. The bias voltage was 12 V_{pp} at 10 kHz across the vertical gap of $120 \mu\text{m}$. (e) An image to measure the ratios of cell alignment. The aligned cells were marked with arrows and the contrasts of brightness (%) were represented. (f) The ratios of cell alignment according to the light contrast were measured at midpoint of alignment for 10 s with a static image pattern. At least five replicates were conducted.

[Fig. 3(e)]. The aligned cells were marked with arrows, while free swimming cells were unmarked. The ratio of cell alignment according to the light contrast was calculated in each area using following definition: (alignment ratio) = (number of aligned cells)/(number of total cells). The alignment ratio increased gradually from 4.3% (at 0% contrast) to greater than 96.0% (at 100% contrast) according to the light contrast [Fig. 3(f)].

To confirm the electric field relationship according to the brightness, we calculated the vertical electric field in the grayscale OET [Fig. 4(a)]. We assumed that the vertical electric field was affected by only the brightness of that pixel and was not affected by the brightness of surrounding area. The brightness was measured to be from 1677 to 43 872 lux at the contrast of brightness was 0%–100%. We get the photoconductivity value of $1.237\text{--}32.377 \mu\text{S}/\text{cm}$ from the measured photoconductivity-brightness relation.⁷ The voltage across the liquid layer was calculated from an equivalent circuit model [see inset of Fig. 4(a)], and the vertical electric field was calculated by dividing the voltage across the liquid layer with the thickness of the liquid layer. The vertical electric field increased according to the brightness and its range was from 35 to $70 \text{ mV}_{\text{pp}}/\mu\text{m}$.

To verify that the direction of the electric field is almost vertical, we compared lateral and vertical electric fields. Figure 4(b) shows a section view according to the dotted line AB in Fig. 3(c). Both lateral and vertical electric fields were calculated using a commercial computational fluid dynamic

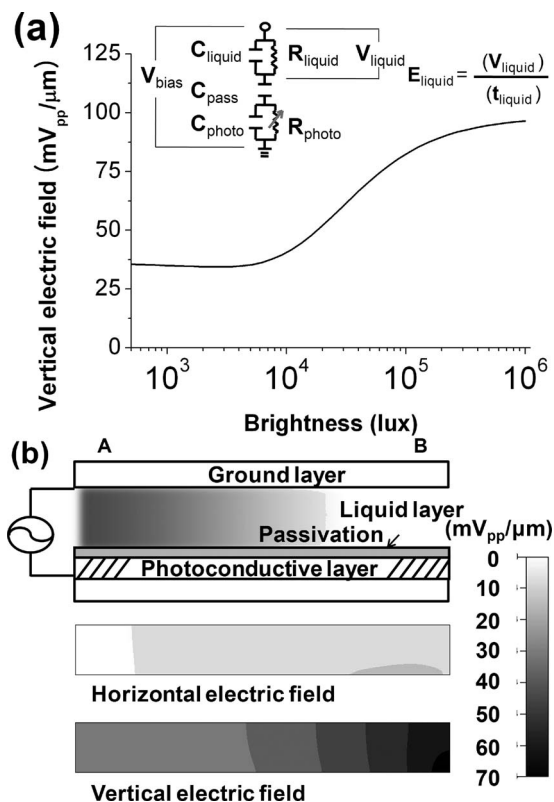


FIG. 4. The calculated electric field distribution. (a) The vertical electric field according to the brightness. The inset represents an equivalent circuit model used to calculate the voltage drop across the liquid layer. (b) The lateral and vertical electric field along the dotted line from A to B in panel c of Fig. 3.

solver (CFD-ACE+, ESI, Huntsville, AL) with the input voltage across the liquid layer. The lateral electric field was 0–10 mV_{pp}/μm, which was less than 1/3 of the vertical electric field at any position. Therefore the maximum angle of the electric field from the vertical direction was less than about $\tan^{-1}(1/3)=18.4^\circ$. In addition, the vertical electric field was almost the same at different height in the liquid layer. However, if the thickness of the liquid layer or grayscale image pattern was changed, the direction of the electric field would not be nearly vertical.

In concern with cell manipulation, we changed only one parameter, the electric field strength, and controlled the others to be unchanged. In addition to the electric field strength, many parameters such as buffer, the shape and properties of cells, and the frequency of electric field will affect electro-orientation. The effect of the frequency and the conductivity of the medium would be complex like that of erythrocytes, which has been studied by Jones,¹² Miller and Jones,¹⁴ and Zimmermann.¹⁷ Detailed experiments and descriptions for the electro-orientation of our model cell are an interesting issue but out of the scope of this study.

The alignment condition used was not so harmful for cells in the experimental range. When the electric field was eliminated, the cells reoriented to its normal shape and swam freely again. However, the cells were damaged when we applied strong electric field, for example over 100 mV_{pp}/μm. Some cells were divided into two or more segments, lysed, and did not get its normal shape or swim freely again even

though the electric field disappeared. These phenomena have been described as deformation and electrical breakdown of the cellular membrane.¹⁷ Therefore we examined the shapes and behavior of cells at the final step in each experiment to confirm that the cells have not been seriously damaged.

It is clear that the grayscale OET is able to control the electric field intensity and has all advantages of the OET. Namely, the OET manipulation can be used not only at a single cell level but also at a multiple-cell level. In addition, the complex, multistep manipulation is possible and the required brightness is much smaller than that of conventional optical tweezers. One of the anticipated applications of this platform is a motility assay of cell. It would be useful to study a signaling pathway of the motile cells by an attractant or a blocker of a specific receptor. These experiments need a single-cell study as well as massively parallel analysis.

In summary, we have developed a grayscale OET which allows adjustment of the electric field strength at each position of OET. The electric field strength was controllable independently in space and time, so that the method was applied to the local alignment of swimming cells. The calculated electric field also showed that the vertical electric field increased according to the brightness. This platform will be a powerful tool in studying cell motility.

This research was supported by the Korea Science and Engineering Foundation (KOSEF) NRL Program grant (R0A-2008-000-20109-0), by the KOSEF grant (R11-2005-008-02003-0), and by the Nano/Bio Science and Technology Program (2005-01291) funded by the Korea government (MEST). The microfabrication works for photoconductive layer were performed at the TFT-LCD Research Center, Kyung Hee University. The first two authors contributed equally to this work.

¹B. Shao, L. Z. Shi, J. M. Nascimento, E. L. Botvinick, M. Ozkan, M. W. Berns, and S. C. Esener, *Biomed. Microdevices* **9**, 361 (2007).

²A. Ashkin, J. M. Dziedzic, and T. Yamane, *Nature (London)* **330**, 769 (1987).

³S. M. Block, D. F. Blair, and H. C. Berg, *Nature (London)* **338**, 514 (1989).

⁴J. M. Nascimento, E. L. Botvinick, L. Z. Shi, B. Durrant, and M. W. Berns, *J. Biomed. Opt.* **11**, 044001 (2006).

⁵P. Y. Chiou, A. T. Ohta, and M. C. Wu, *Nature (London)* **436**, 370 (2005).

⁶Y. Lu, Y. Huang, J. A. Yeh, and C. Lee, *Opt. Quantum Electron.* **37**, 1385 (2005).

⁷W. Choi, S. H. Kim, J. Jang, and J. K. Park, *Microfluid. Nanofluid.* **3**, 217 (2007).

⁸H. Hwang, Y. Oh, J. J. Kim, W. Choi, J. K. Park, S. H. Kim, and J. Jang, *Appl. Phys. Lett.* **92**, 024108 (2008).

⁹A. Jamshidi, P. J. Pauzauskie, P. J. Schuck, A. T. Ohta, P.-Y. Chiou, J. Chou, P. Yang, and M. C. Wu, *Nat. Photonics* **2**, 86 (2008).

¹⁰S. Park, C. Pan, T. H. Wu, C. Kloss, S. Kalim, C. E. Callahan, M. Teittel, and E. P. Y. Chiou, *Appl. Phys. Lett.* **92**, 151101 (2008).

¹¹H. Hwang, Y. J. Choi, W. Choi, S. H. Kim, J. Jang, and J. K. Park, *Electrophoresis* **29**, 1203 (2008).

¹²T. B. Jones, *Electromechanics of Particles* (Cambridge University Press, Cambridge, 1995).

¹³T. B. Jones, *IEEE Eng. Med. Biol. Mag.* **22**, 33 (2003).

¹⁴R. D. Miller and T. B. Jones, *Biophys. J.* **64**, 1588 (1993).

¹⁵J. W. Choi, A. Pu, and D. Psaltis, *Opt. Express* **14**, 9780 (2006).

¹⁶See EPAPS Document No. E-APPLAB-93-091840 for a movie clip in mpeg format. For more information on EPAPS, see <http://www.aip.org/pubservs/epaps.html>.

¹⁷U. Zimmermann, *Biochim. Biophys. Acta* **694**, 227 (1982).